Massive Stars Across Redshifts in the Era of JWST and Large Surveys
Proceedings IAU Symposium No. 402, 2026
A. Wofford, N. St Louis, M. García, S. Simón-Díaz & L. M. Oskinova, eds.
doi:10.1017/S1743921326106309

Stellar population synthesis models including binary stars

G. Bruzual[1], M. Lecroq[2], S. Charlot[2], A. Bressan[3,4], G. Costa[4,5], G. Iorio[7], M. Spera[3,8,9], M. Mapelli[4,5,6,10], Y. Chen[11,12], J. Chevallard[13] and M. Dall'Amico[5,6,10]

[1]Instituto de Radioastronomía y Astrofísica, UNAM, Campus Morelia, Michoacán, México, C.P. 58089, México
email: g.bruzual@irya.unam.mx

[2]Sorbonne Université, CNRS, UMR 7095, Institut d'Astrophysique de Paris, 98 bis bd Arago, F-75014 Paris, France

[3]SISSA, via Bonomea 265, I-34136 Trieste, Italy

[4]INAF, Osservatorio Astronomico di Padova, Vicolo dell'Osservatorio 5, I-35122 Padova, Italy

[5]Dipartimento di Fisica e Astronomia Galileo Galilei, Università di Padova, Vicolo dell'Osservatorio 3, I-35122 Padova, Italy

[6]INFN-Padova, Via Marzolo 8, I-35131 Padova, Italy

[7]Departament de Física Quàntica i Astrofísica, Institut de Ciències del Cosmos, Universitat de Barcelona, Martí i Franquès 1, E-08028 Barcelona, Spain

[8]INAF, Osservatorio Astronomico di Roma, Via Frascati 33, I-00040 Monteporzio Catone, Italy

[9]INFN-Trieste, Via Valerio 2, I-34127 Trieste, Italy

[10]Universität Heidelberg, Zentrum für Astronomie, Institut für Theoretische Astrophysik, Albert-Ueberle-Str 2, D-69120 Heidelberg, Germany

[11]School of Physics and Optoelectronic Engineering, Anhui University, Hefei 230601, China

[12]National Astronomical Observatories, Chinese Academy of Sciences, Beijing 100101, China

[13]Department of Physics, University of Oxford, Denys Wilkinson Building, Keble Road, Oxford OX1 3RH, UK

Abstract. I present a few results from the GALSEVN stellar population synthesis models that include the evolution of massive binary stars that are of interest for the audience of this symposium.

Keywords. Stellar populations, Binary stars, Distant galaxies, Spectral evolution, Galaxy evolution

1. Introduction

The JWST has revealed the existence of large number of galaxies at high redshift, in excess of $z = 14$. Many of these galaxies are expected to be young galaxies in the reionization-era. In the rest-frame these galaxies are observed in the ultraviolet (UV) with exquisite signal-to-noise-ratio. The interpretation of these data requires reliable predictions of the UV properties of young and metal poor stellar populations. Single star stellar population synthesis models (e.g., Bruzual & Charlot 2003) most likely under-predict the UV-flux and number of ionizing photons for these populations, hampering

© The Author(s), 2026. Published by Cambridge University Press on behalf of The International Astronomical Union. This is an Open Access article, distributed under the terms of the Creative Commons Attribution licence (https://creativecommons.org/licenses/by/4.0/), which permits unrestricted re-use, distribution and reproduction, provided the original article is properly cited.

https://doi.org/10.1017/S1743921326106309 Published online by Cambridge University Press

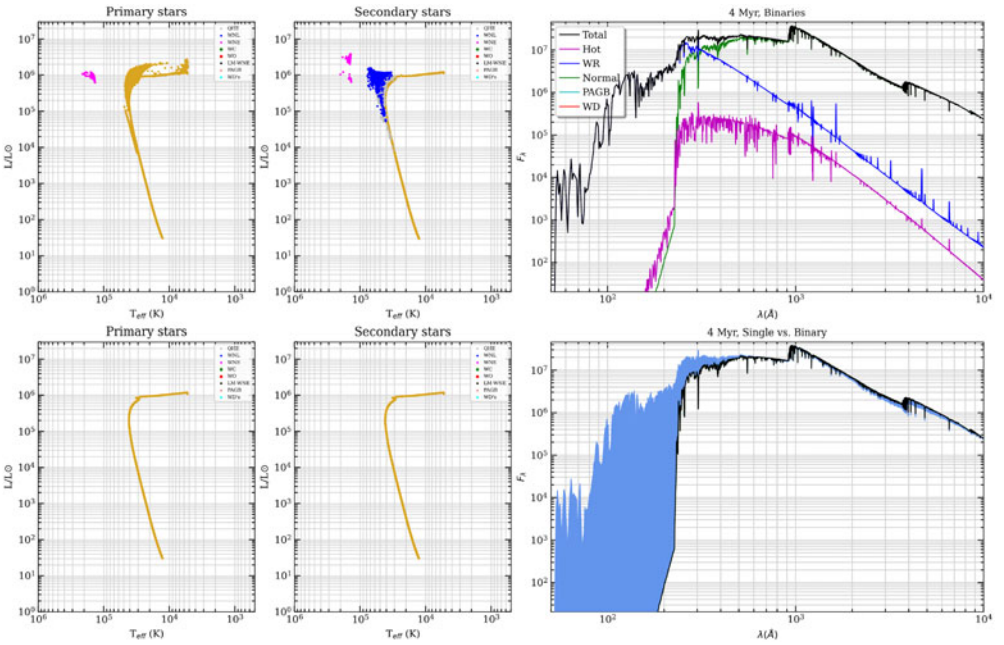


Figure 1. Same as Figure 3 but for 4 Myr.

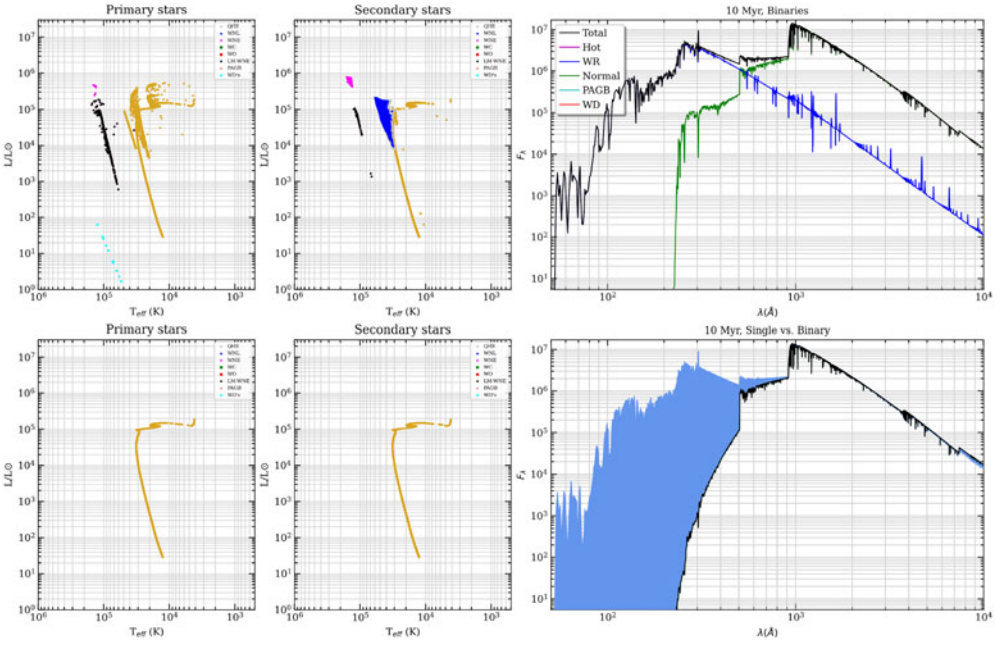


Figure 2. Same as Figure 3 but for 10 Myr.

detailed studies of the emission-line properties of these galaxies. It is well established by now that population synthesis models that include the presence of interacting (mass exchanging) massive binary stars predict higher UV fluxes and larger number of ionizing photons and massive stars that last for longer periods of time than single star models, e.g., BPASS (Stanway & Eldridge 2018), MESA (MESA team) and GALSEVN (Lecroq

https://doi.org/10.1017/S1743921326106309 Published online by Cambridge University Press

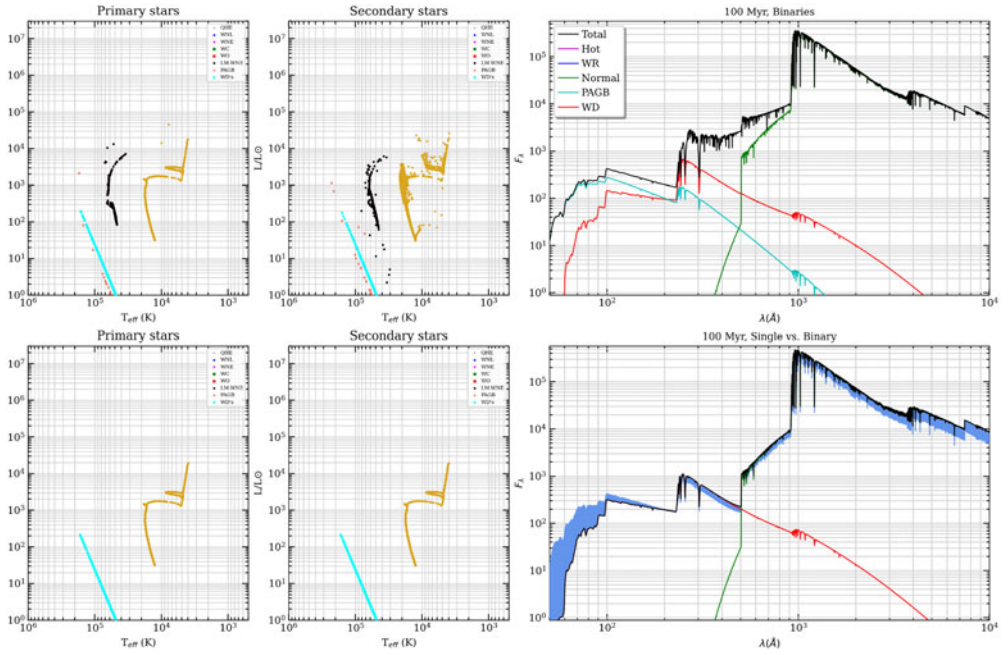


Figure 3. 100 Myr isochrones in the HRD described by the primary (LHS panels) and secondary stars (central panels) in the $Z = 0.001$ GALSEVN model. The corresponding SED in the range from 50 Å to 1 μm is shown in the RHS panels. The binary pairs in the *bottom* panels are evolved as single stars, suppressing mass transfer between them, which is apparent from the differences in the isochrones in the *top* ($\mathcal{B} = 1$ model, see below) and *bottom* ($\mathcal{B} = 0$ model) panels. The *blue* shaded area in the *bottom* RHS panel shows the difference in the UV range shortward of 912 Å between the GALSEVN SED including binary evolution (*black* line in the *top* RHS panel) and the corresponding SED when stars are evolved as single (*black* line in the *bottom* RHS panel). The contribution to the SED of stars of different groups is shown in the RHS panels. Not all groups contribute at all ages, cf. Figures 1, 2 and 6.

et al. 2024) models. Due to lack of space, only a few results from the GALSEVN models of interest for the audience of this symposium are discussed in this paper.

2. GALSEVN models

We study the spectral evolution of stellar populations that include single and binary stars by combining the GALAXEV (Bruzual & Charlot 2003; Plat et al. 2019, CB19 hereafter) and the SEVN (Spera et al. 2015; Spera & Mapelli 2017; Spera et al. 2019; Mapelli et al. 2020; Iorio et al. 2023) codes. The open-source code SEVN interpolates on the fly the stellar properties of each companion in a binary pair from available evolutionary tracks for single stars, PARSEC (Chen et al. 2015) in our case, making it faster and more flexible than other binary stellar evolution codes like BPASS or MESA that follow the detailed evolution of each star in the pair. The SEVN code provides the position in the HR-diagram (HRD) at different ages of binary pairs with initial primary and secondary star mass (m_1, m_2), where $2 \leq m_1 \leq 300\, M_\odot$ and $m_2 = q m_1$. For q we adopt the probability density function $\mathrm{PDF}(q) \propto q^{-1}$ with $q \in [0.1, 1]$ as in Sana et al. (2012). To each of these stars we assign the corresponding spectral energy distribution (SED) using the GALAXEV compilation of stellar spectral libraries listed in (Sánchez et al. 2022, tables 8 to 12). Additionally, for main sequence stars hotter than $T_{eff} = 50,000$ K we use the WM-BASIC spectral models computed by Chen et al. (2015). The resulting

https://doi.org/10.1017/S1743921326106309 Published online by Cambridge University Press

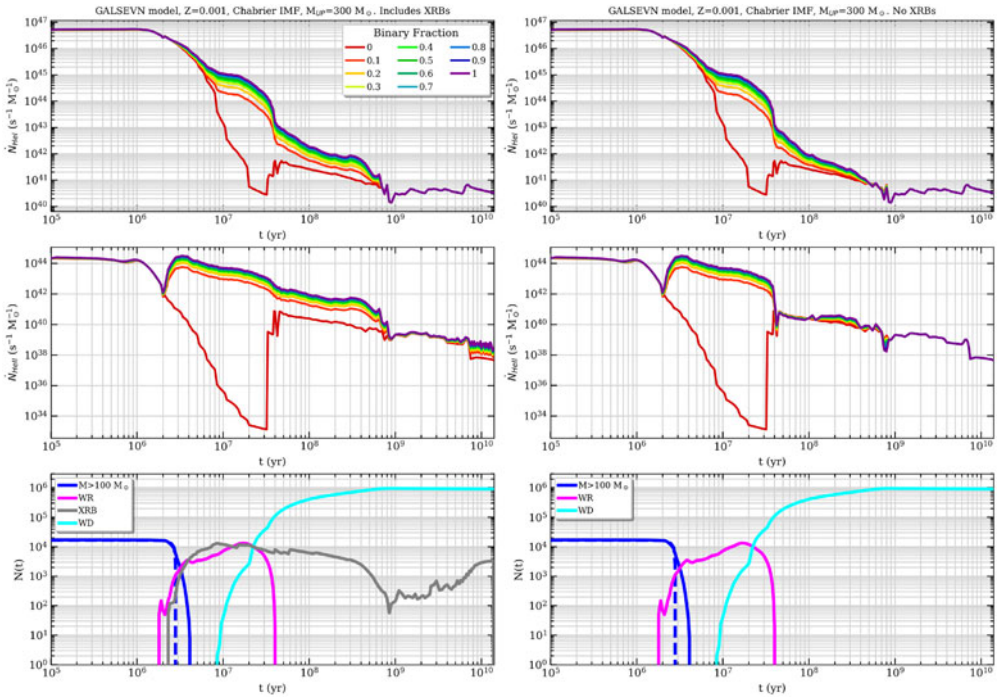


Figure 4. Production rate of He I and He II ionizing photons per unit stellar mass vs. age for $Z = 0.001$ GALSEVN models for $\mathcal{B} \in [0, 1]$. The panels on the LHS/RHS include/exclude the emission by accretion discs around XRBs. The two *bottom* panels show the number of stars of various types responsible for producing the ionizing photons in the $\mathcal{B} = 1$ model. The *dashed* − *blue* line corresponds to the $\mathcal{B} = 0$ model. The excess of massive stars in the $\mathcal{B} = 1$ model and the role played by the XRB disks are clearly noticeable.

models are dubbed GALSEVN models (Lecroq et al. 2024). The GALSEVN models also include the emission by hot accretion discs formed around X-ray binaries (XRBs) where a compact object (neutron star or stellar-mass black hole) accretes material from a companion. The GALSEVN models have been computed for 15 different values of the stellar metallicity Z ranging from $Z = 10^{-11}$ to $Z = 0.04$. Results are presented here only for the $Z = 0.001$ GALSEVN model, computed for one million binary pairs. For more details on the GALSEVN models see Lecroq et al. (2024, 2025).

Figures 1, 2 and 3 show the isochrones in the HRD described by the primary and secondary stars in the $Z = 0.001$ GALSEVN model at 4, 10, and 100 Myr, respectively, together with the resulting SED in the range from 50 Å to 1 μm. For the *bottom* panels in these figures, the stars in each pair are evolved as single stars, suppressing mass transfer between them, which is apparent from the differences in the isochrones in the *top* and *bottom* panels. The *blue* shaded area in the *bottom* RHS panels of these figures show the difference in the UV range shortward of 912 Å between the GALSEVN SED including binary evolution (*black* line in the *top* RHS panel) and the corresponding SED when stars are evolved as single (*black* line in the *bottom* RHS panel). The contribution to the SED of different stellar groups is shown in the RHS panels of these Figures. Not all groups contribute at all ages, cf. Figures 1, 2 and 6. See captions to Figures 3 and 6.

Combining the $\mathcal{B} = 1$ (100% binary) and the $\mathcal{B} = 0$ (100% single) star models in the *top* and *bottom* panels of Figures 1, 2 and 3, respectively, we can model stellar populations

https://doi.org/10.1017/S1743921326106309 Published online by Cambridge University Press

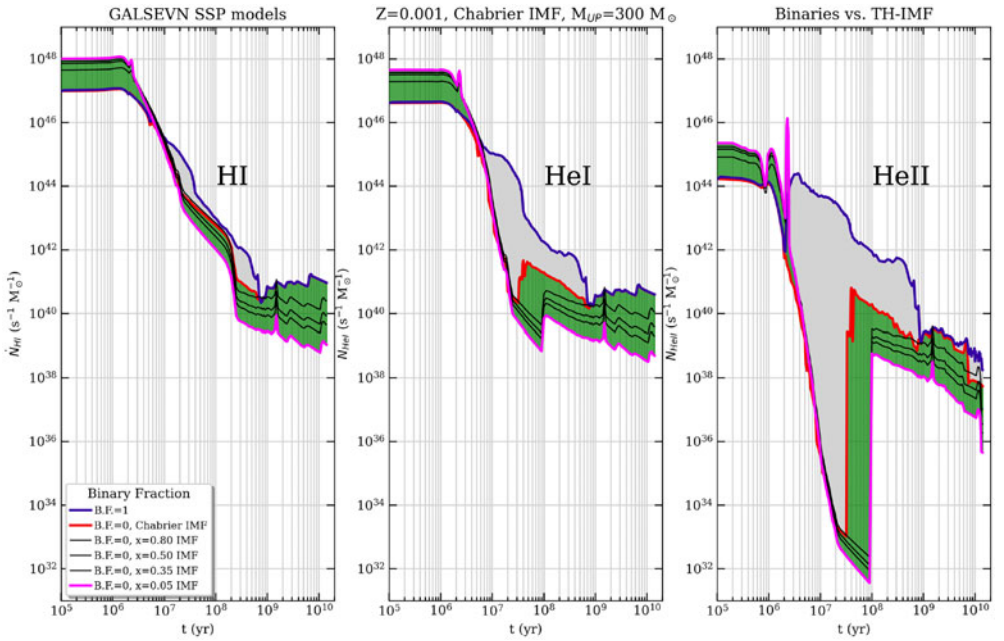


Figure 5. Comparison of the production rate of H I, He I and He II ionizing photons vs. age for the $\mathcal{B}=1$ $Z=0.001$ GALSEVN model (Lecroq et al. 2024) and CB19 GALAXEV models computed for the Chabrier IMF and 4 different top-heavy IMFs, as indicated in the legend in LHS panel. The *green* shaded area indicates the range covered by the top-heavy IMF models. The *gray* shaded area shows the excess of photons in the GALSEVN model with respect to the Chabrier IMF GALAXEV model.

with an arbitrary *binary fraction* $\mathcal{B}$.† Figure 4 shows the production rate of He I and He II ionizing photons vs. age for $Z=0.001$ GALSEVN models with $\mathcal{B}\in[0,1]$ (Lecroq et al. 2024). The panels on the LHS/RHS include/exclude the emission by accretion discs around XRBs. The two *bottom* panels show the number of stars of various types in the $\mathcal{B}=1$ model responsible of producing the ionizing photons.

Figure 5 compares the production rate of H I, He I and He II ionizing photons vs. age for the $\mathcal{B}=1$ $Z=0.001$ GALSEVN model (Lecroq et al. 2024) with CB19 GALAXEV models computed for the Chabrier IMF and 4 different top-heavy IMFs, as indicated in the LHS panel. As expected, at early ages (below a few Myr) the top-heaviest IMF model produces more ionizing photons than the other models. As binary interactions set in, the production rate of ionizing photons by the GALSEVN model exceeds that of the Chabrier and the top-heavy IMF models.

Figure 6 shows the contribution of different stellar groups to the total SED in the $\mathcal{B}=1$ and $\mathcal{B}=0$ GALSEVN models in the age range from 0.7 to 500 Myr. WR and stars hotter than 50,000 K that have an important contribution in the $\mathcal{B}=1$ model are absent in the $\mathcal{B}=0$ model. Figure 7 shows that no WR stars are formed in the GALSEVN model when binary pairs are evolved as single stars ($\mathcal{B}=0$). Figure 8 compares the number distribution of massive stars ($m\geq 100\,M_\odot$) vs. age for both models. By construction, no stars with $m\geq 300\,M_\odot$ are present in the $\mathcal{B}=0$ model but there are plentiful of them, formed in binary interactions, in the $\mathcal{B}=1$ model at early ages.

† Following Kouwenhoven et al. (2009) and Reipurth & Zinnecker (1993), $\mathcal{B}=\frac{B}{S+B}$, where S and B are the number of single and binary stars, respectively. The number of systems is then $\mathcal{S}=S+B$ and the total number of (individual) stars is $\mathcal{N}=S+2B$.

https://doi.org/10.1017/S1743921326106309 Published online by Cambridge University Press

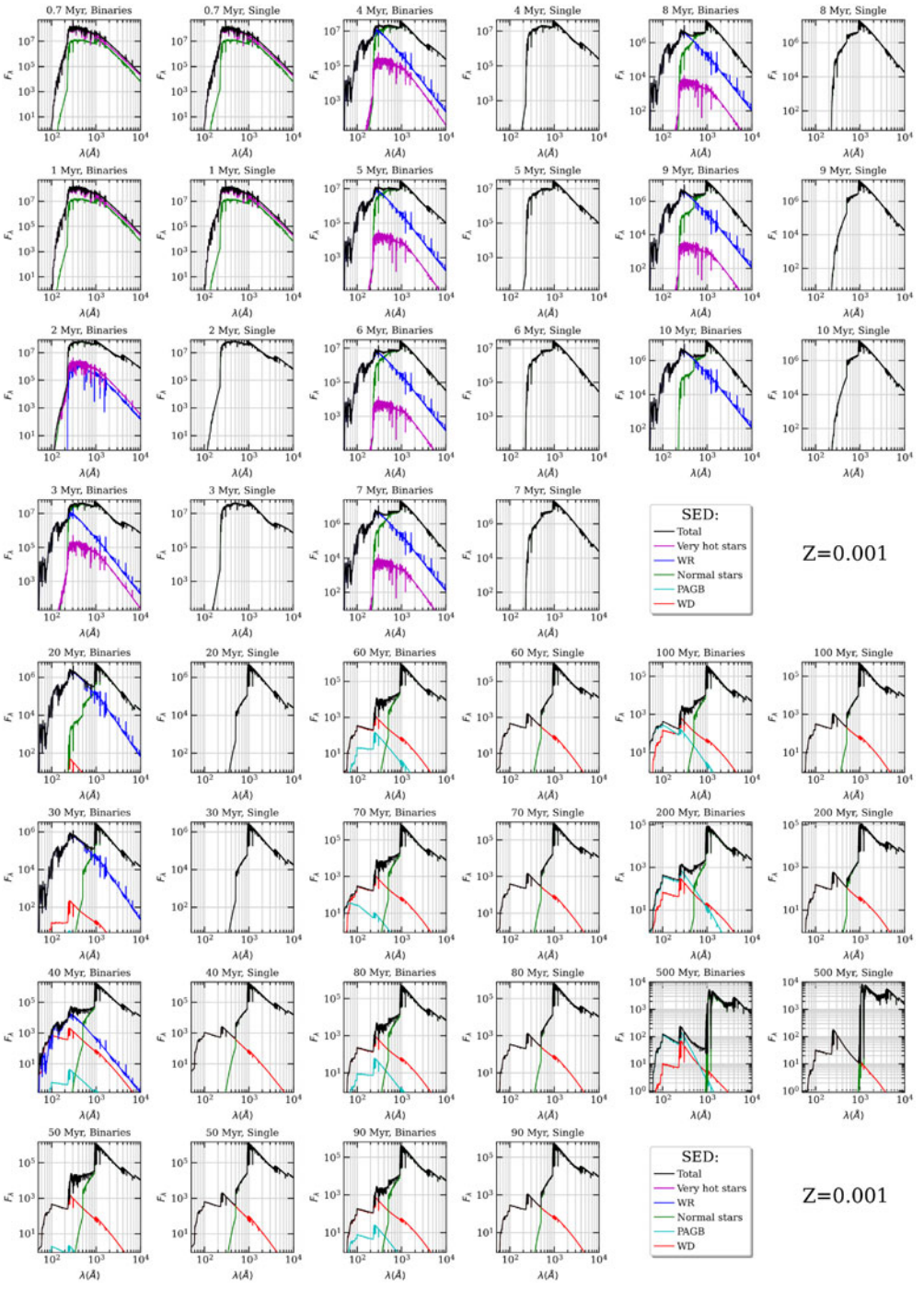


Figure 6. Contribution of different stellar groups to the total SED in the $\mathcal{B}=1$ (*odd* column panels) and the $\mathcal{B}=0$ (*even* column panels) GALSEVN models in the age range from 0.7 to 500 Myr (from *top* to *bottom*). WR stars (in *blue*) and stars hotter than 50,000 K (in *magenta*) that have an important contribution in the $\mathcal{B}=1$ model are absent in the $\mathcal{B}=0$ model. As shown in Figure 7, no WR stars are formed when binary pairs are evolved as single stars ($\mathcal{B}=0$). Massive stars ($m \geq 300\,M_{\odot}$), formed in binary interactions in the $\mathcal{B}=1$ model at early ages, are responsible of the *magenta* SED denoted *very hot stars*. Age is indicated at the top of each panel

https://doi.org/10.1017/S1743921326106309 Published online by Cambridge University Press

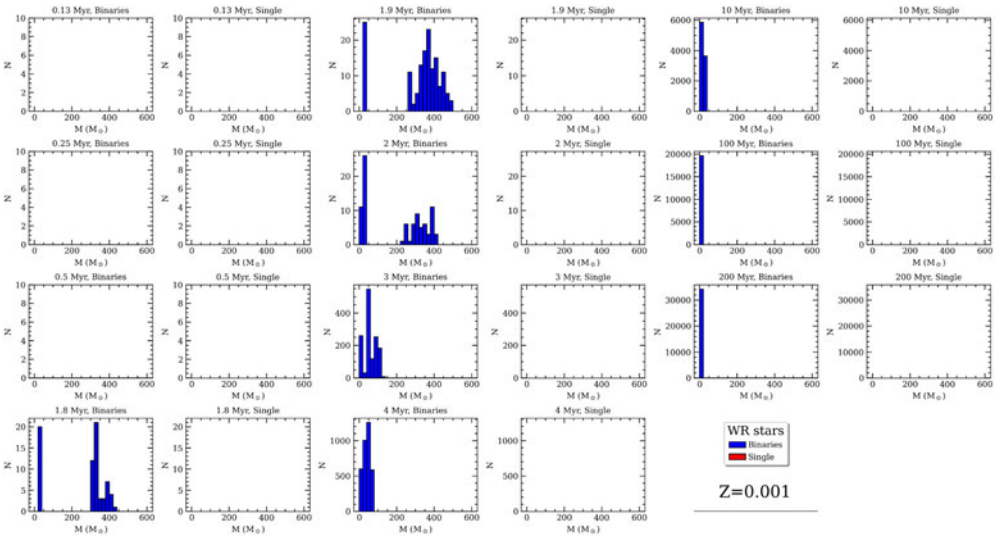


Figure 7. Number distribution of WR stars vs. age for the $\mathcal{B}=1$ (*blue* histograms) and $\mathcal{B}=0$ (*red* histograms) GALSEVN models. No WR stars appear when the binary pairs are evolved as single stars ($\mathcal{B}=0$) according to the tracks used in the GALSEVN models for $Z=0.001$. Age is indicated at the top of each panel.

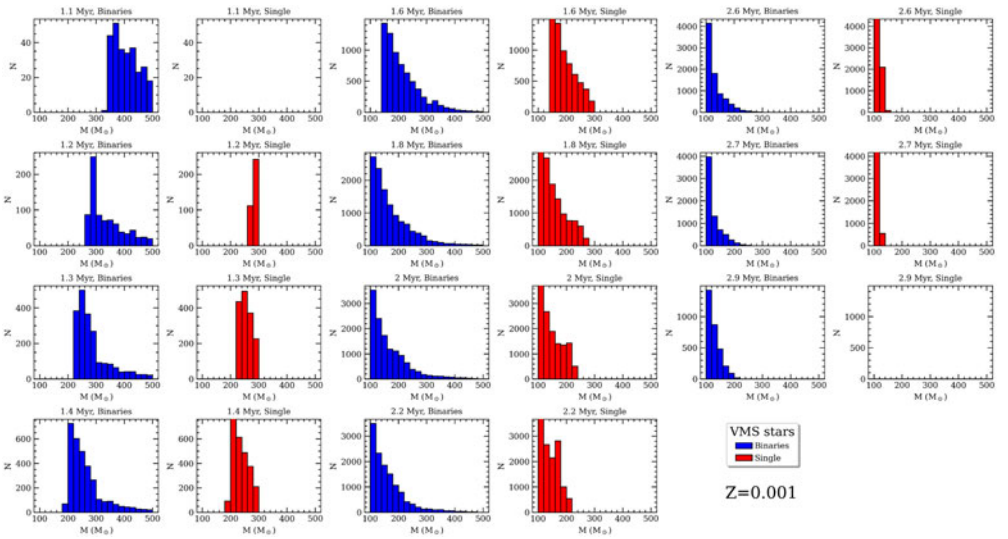


Figure 8. Number distribution of massive stars ($m \geq 100\,M_{\odot}$) vs. age for the $\mathcal{B}=1$ (*blue* histograms) and $\mathcal{B}=0$ (*red* histograms) GALSEVN models. By construction, no stars with $m \geq 300\,M_{\odot}$ (upper mass limit of the IMF) exist in the $\mathcal{B}=0$ model, but many of them are formed by binary interactions in the $\mathcal{B}=1$ model at early ages. Age is indicated at the top of each panel.

https://doi.org/10.1017/S1743921326106309 Published online by Cambridge University Press

3. Summary

Including the evolution of interacting massive binary star pairs in population synthesis models introduces important differences in the SEDs of young stellar populations, especially in the UV range below 912 Å. It is important that this kind of models are used when interpreting data of young galaxies, possibly seen in the reionization-era. Some applications of the GALSEVN models are discussed in Lecroq et al. (2024, 2025).

References

Bruzual, G. & Charlot, S. 2003, *MNRAS*, 344, 4, 1000.
Chen, Y., Bressan, A., Girardi, L., et al. 2015, *MNRAS*, 452, 1, 1068.
Iorio, G., Mapelli, M., Costa, G., et al. 2023, *MNRAS*, 524, 1, 426.
Kouwenhoven, M. B. N., Brown, A. G. A., Goodwin, S. P., et al. 2009, *A&A*, 493, 3, 979.
Lecroq, M., Charlot, S., Bressan, A., et al. 2024, *MNRAS*, 527, 3, 9480.
Lecroq, M., Charlot, S., Bressan, A., et al. 2025, *A&A*, 695, A17.
Mapelli, M., Spera, M., Montanari, E., et al. 2020, *ApJ*, 888, 2, 76.
Plat, A., Charlot, S., Bruzual, G., et al. 2019, *MNRAS*, 490, 1, 978.
Reipurth, B. & Zinnecker, H. 1993, *A&A*, 278, 81.
Sana, H., de Mink, S. E., de Koter, A., et al. 2012, Science, 337, 6093, 444.
Sánchez, S. F., Barrera-Ballesteros, J. K., Lacerda, E., et al. 2022, *ApJS*, 262, 2, 36.
Spera, M., Mapelli, M., & Bressan, A. 2015, *MNRAS*, 451, 4, 4086.
Spera, M. & Mapelli, M. 2017, *MNRAS*, 470, 4, 4739.
Spera, M., Mapelli, M., Giacobbo, N., et al. 2019, *MNRAS*, 485, 1, 889.
Stanway, E. R. & Eldridge, J. J. 2018, *MNRAS*, 479, 1, 75.

https://doi.org/10.1017/S1743921326106309 Published online by Cambridge University Press